Nuclear moments of the first excited state of ^{22}Ne from ^{22}Ne(132 MeV)+^{208}Pb scattering

E. E. Gross, T. P. Cleary, J. L. C. Ford, Jr., D. C. Hensley, and K. S. Toth
Oak Ridge National Laboratory, Oak Ridge, Tennessee 37830

F. T. Baker and A. Scott
University of Georgia, Athens, Georgia 30602

C. R. Bingham and J. A. Vrba
University of Tennessee, Knoxville, Tennessee 37916
(Received 6 September 1983)

Elastic and inelastic cross section data for exciting the ^{22}Ne 2_1^+ (1.27 MeV) state by 132 MeV ^{22}Ne scattering from a ^{208}Pb target are presented. The data are analyzed by a rotational model coupled-channels calculation including the 0^+ ground state and the 2_1^+, and 4_1^+ states of ^{22}Ne. We extract β_2 and β_4 deformation parameters, as well as $M(E2;0^+\text{-}2_1^+)$, $M(E2;2_1^+\text{-}2_1^+)$, $M(E4;0^+\text{-}4_1^+)$, and $M(E2;2_1^+\text{-}4_1^+)$ matrix elements for ^{22}Ne and compare these quantities to those obtained for ^{20}Ne. The extracted 2_1^+ reorientation matrix element is considerably larger than shell-model predictions. Addition of a negative spin-orbit potential improves the fit to the 2_1^+ differential cross section.

NUCLEAR REACTIONS ^{208}Pb(^{22}Ne,^{22}Ne), ^{208}Pb(^{22}Ne,^{22}Ne′) $E_{\rm lab}=132$ MeV, measured $\sigma(\theta)$; deduced optical potential, quadrupole and hexadecapole deformation parameters and transition matrix elements of ^{22}Ne by a coupled-channels analysis. Enriched target.

I. INTRODUCTION

Coupled-channels analyses of heavy-ion inelastic-scattering data taken at energies slightly above the Coulomb barrier have proven useful in providing collective nuclear-structure properties. Examples include β_4 deformations,[1,2] static quadrupole moments of 2^+ states,[3,4] triaxial shape parameters,[5,6] and the relative phases of matrix elements.[4,7] In cases where the collective model was too restrictive, a semimicroscopic approach succeeded in obtaining insight into cluster properties of nuclear wave functions.[8,9] Analysis of such data has also played a role in determining properties of the ion-ion optical potential. At energies slightly above the Coulomb barrier the elastic scattering is primarily sensitive to the real potential in the neighborhood of the strong absorption radius,[10] but strongly coupled excited states have to be accounted for prior to deducing optical model parameters.[11] Inelastic scattering together with transfer reactions has a bearing on the surface transparency of the ion-ion optical potential.[12] The need for a spin-dependent potential has been directly demonstrated by asymmetry measurements of elastically scattered aligned ^{6}Li nuclei.[13] Recently, further evidence for such a term has been suggested by analysis of m-substate populations following inelastic scattering[14] and by reaction asymmetries following single nucleon transfer.[15]

In this paper, we present new elastic and inelastic (^{22}Ne, 1.27 MeV 2_1^+ state) scattering data for 132-MeV ^{22}Ne incident on a ^{208}Pb target. The data are subjected to a rotational-model coupled-channels analysis from which we extract optical model potential parameters and transition matrix elements. The data and analysis complement those previously reported[2] for ^{20}Ne scattering from a ^{208}Pb target at the same center of mass energy.

II. EXPERIMENTAL DETAILS AND RESULTS

A 132.2±0.1 MeV ^{22}Ne^{6+} beam was provided by the Oak Ridge isochronous cyclotron. The target consisted of 220 μg/cm^2 ^{208}Pb (99.1% enriched) evaporated onto a 40-μg/cm^2 carbon foil. The energy at the center of the Pb target was estimated to be 132.0±0.2 MeV. Scattered particles were observed with a position-sensitive solid-state detector located on a movable arm within a 76-cm diameter scattering chamber. A fifteen-element slit in front of the detector defined 0.5° angular apertures centered at 1° intervals. Starting at 20° laboratory, the detector was moved five times in 10° steps, thus overlapping five angles of the previous setting. This procedure results in smooth, well-defined angular distributions. The overall energy resolution was 500 keV, which required careful unfolding of the ^{22}Ne (1.27 MeV) 2_1^+ state from elastic scattering at the more forward angles. The absolute normalization was obtained by normalizing $\sigma^{0^+}+\sigma^{2^+}$ (^{22}Ne) + σ^{3^-} (^{208}Pb) to the calculated Rutherford cross section for the Coulomb dominated region, $\theta_{\rm c.m.}\leq 35°$. Further experimental details as well as the method of data acquisition and data reduction may be found in Ref. 16.

Elastic scattering as a ratio to Rutherford scattering is shown as closed circles in Fig. 1. Also shown in Fig. 1 as open circles are the previous data for ^{20}Ne(131

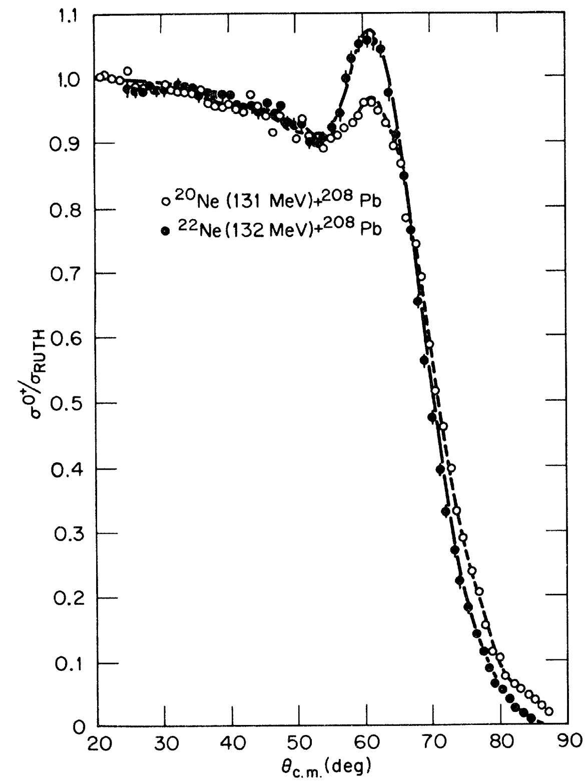

FIG. 1. ^{22}Ne(132 MeV) + ^{208}Pb elastic scattering relative to Rutherford as solid circles and similar data for ^{20}Ne(131 MeV) + ^{208}Pb as open circles (Ref. 2). The curves are coupled-channels fits including 0^+, 2_1^+, and 4_1^+ states. Parameters corresponding to the fits are contained in Tables I—III.

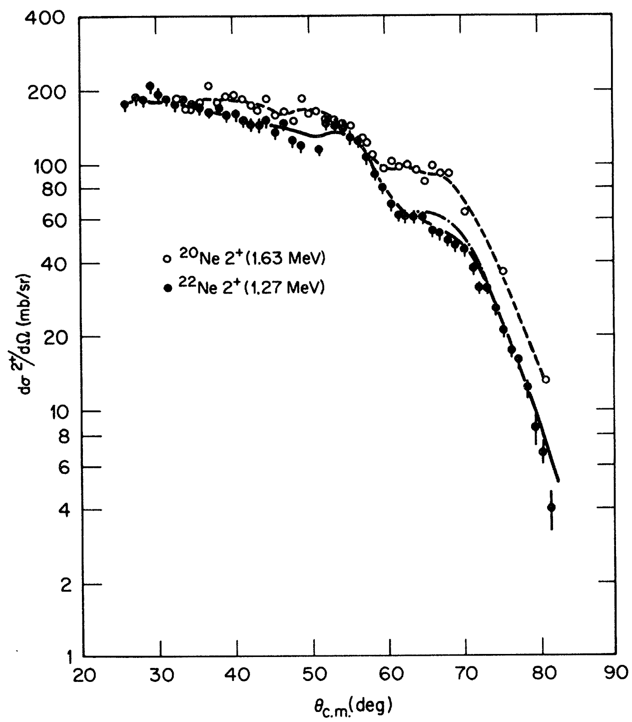

FIG. 2. Differential cross sections for exciting the ^{22}Ne 2_1^+ state (1.27 MeV), solid circles, and the ^{20}Ne 2_1^+ state (1.63 MeV), open circles, by scattering from a ^{208}Pb target at 119.5 MeV c.m. The solid and dashed curves are minimum χ^2 coupled-channels fits corresponding to the elastic scattering fits in Fig. 1. The dotted-dashed curve is the best fit obtained for the ^{22}Ne data without a spin-orbit term in the optical potential. Parameters for these fits are summarized in Tables I—III.

MeV) + ^{208}Pb elastic scattering.[2] The effect of a larger cross section for the ^{20}Ne 2_1^+ state relative to that of the ^{22}Ne 2_1^+ state (see Fig. 2) in suppressing the elastic scattering peak near 65° c.m. is clearly seen. A similar comparison for the 2_1^+ state differential cross sections is displayed in Fig. 2 again as closed circles for ^{22}Ne and open circles for ^{20}Ne. A striking difference is apparent in the behavior of the 2_1^+ differential cross sections in the neighborhood of $\theta_{c.m.} \approx 65°$. In the case of ^{20}Ne this behavior suggested the presence of a large positive hexadecapole moment in the ^{20}Ne ground state wave function.[2] As is discussed below, the ^{22}Ne 2_1^+ cross section is consistent with a small negative β_4 deformation, but the analysis also suggests the need for a spin-orbit term in the ion-ion potential for the ^{22}Ne + ^{208}Pb system to account for the behavior of $\sigma^{2_1^+}$ near 65° c.m.

III. ANALYSIS

The rotational-model coupled-channels analysis of the present ^{22}Ne + ^{208}Pb data follows closely that of the prior ^{20}Ne + ^{208}Pb analysis.[2] Woods-Saxon form factors with β_2 and β_4 deformations were used and all multipole orders in the couplings were included. The calculations were performed using the automatic search program ECIS-79.[17] Most of the calculations included the $0^+ \leftrightarrow 2_1^+ \leftrightarrow 4_1^+$ couplings shown in Fig. 3. A few calculations were also performed which included the ^{22}Ne 2_2^+ state at 4.46 MeV. We allowed the $2_1^+ \leftrightarrow 2_2^+$ coupling to vary ±50% from the adopted $M(E2)$ value[18] and varied the signs of both $M(E2;0_1^+\text{-}2_1^+)$ and $M(E2;2_1^+\text{-}2_2^+)$. These calculations did not show enough sensitivity to the 2_1^+ differential cross section to determine either the magnitude of the matrix elements or to deduce the sign[4,7] of

$$p_4 = M_{0_12_1} M_{0_12_2} M_{2_12_1} M_{2_12_2} ,$$

where

$$M_{ij} = -\langle i || M(E2) || j \rangle .$$

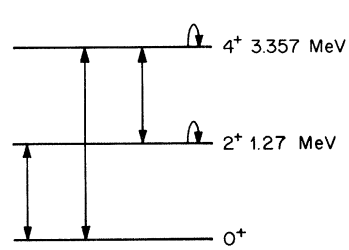

FIG. 3. Rotational-model transitions included in the 0^+, 2_1^+, and 4_1^+ coupled-channels calculations. All multipole orders in the couplings were included. Matrix elements were allowed to vary from their rotational-model values to fit the data.

TABLE I. Optical model parameters for 0^+, 2_1^+, and 4_1^+ coupled-channels fits to ^{20}Ne (131 MeV) and ^{22}Ne (132 MeV) scattering from ^{208}Pb. The Thomas form spin-orbit potential was taken to have the same geometry parameters as the real potential. The Coulomb radius parameter was $r_C = 1.25$ fm.

	V (MeV)	r_V (fm)	a_V (fm)	W (MeV)	r_W (fm)	a_W (fm)	V_{LS} (MeV)
^{20}Ne	21.50	1.34	0.485	7.81	1.43	0.300	0
^{22}Ne	18.91	1.34	0.565	4.58	1.43	0.361	−0.16

Inclusion of the 6^+ state (6.31 MeV) with rotational model couplings was also tried and found to have an insignificant influence on the calculated 2_1^+ cross section.

We started with the optical potential which successfully fitted the previous[2] $^{20}\mathrm{Ne} + {}^{208}\mathrm{Pb}$ data at 130 MeV; $V = 21.5$ MeV, $r_V = 1.34$ fm, $a_V = 0.49$ fm, $W = 7.0$ MeV, $r_W = 1.43$ fm, $a_W = 0.30$ fm, $r_C = 1.25$ fm, and no spin-orbit term. The initial calculations used electron scattering values[19] for $M(E2;0^+\text{-}2_1^+)$, a lifetime measurement[20] to obtain $M(E2;2_1^+\text{-}4_1^+)$, a Coulomb excitation value[21] for the reorientation matrix element $M(E2;2_1^+\text{-}2_1^+)$, and a value for $M(E4;0^+\text{-}4_1^+)$ taken from proton inelastic scattering.[22]. All matrix elements were subsequently allowed to vary to obtain a minimum χ^2 fit. The reorientation matrix element for the 4_1^+ state, $M(E2;4_1^+\text{-}4_1^+)$, exerted very little influence on the calculated 2_1^+ cross section, and it was therefore fixed at the rotational model value. Nuclear form factors (deformation lengths) were related to the Coulomb parameters using the rolling-model scaling procedure.[23] Decoupling nuclear deformation lengths from the rolling model values resulted in only slightly improved fits.

The above parameters gave a fair representation of the 2_1^+ differential cross section except in the angular region $60° \leq \theta_{\mathrm{c.m.}} \leq 70°$, where deviation of the calculation from the data unduly influenced the search on the real potential. We therefore limited the search on V and a_V to the 0^+ data and fixed their values in all subsequent searches. All other searches included both 0^+ and 2_1^+ data of Figs. 1 and 2. W and a_W are then most sensitive to the exponential falloff of the elastic scattering; $M(E2;0^+\text{-}2_1^+)$ is most sensitive to the magnitude of the 2_1^+ cross section in the angular region $\theta_{\mathrm{c.m.}} \lesssim 50°$; $M(E2;2_1^+\text{-}2_1^+)$ is primarily determined by the behavior of $\sigma^{2_1^+}$ in the region $\theta_{\mathrm{c.m.}} \gtrsim 70°$; whereas $M(E2;0^+\text{-}4_1^+)$ and $M(E2;2_1^+\text{-}4_1^+)$ primarily influence $\sigma^{2_1^+}$ in the problem region of $60° \lesssim \theta_{\mathrm{c.m.}} \lesssim 70°$. As is shown in detail in Ref. 2, it is this separation of sensitivities, as well as the availability of high quality angular distributions throughout the Coulomb-nuclear interference region, that allows a coupled-channels analysis to determine the parameters in a less ambiguous way.

The best fit to the data is represented by the solid curves in Figs. 1 and 2. Corresponding optical model parameters are shown in Table I, deformation parameters in Table II, and matrix elements in Table III. The errors given on our results for the ^{22}Ne matrix elements represent subjective judgments as to the limits of an acceptable fit. Included in the optical potential is a small negative spin-orbit term ($V_{LS} = -0.16$ MeV) of the Thomas form and with the same geometry parameters as the real potential. The spin is that of the ^{22}Ne 2_1^+ state and no spin-orbit term is included in the transition potential. Without this term, the best fit to $\sigma^{2_1^+}$ has a 50% larger χ^2 value and is shown as the dotted-dashed curve in Fig. 2. The extracted matrix elements of Table III are in fair agreement with those obtained by electron scattering,[19] lifetime measurements,[20] and Coulomb excitation.[21,24] In particular, the reorientation matrix element $M(E2;2_1^+\text{-}2_1^+)$ confirms a large value for this quantity[21,24] and emphasizes a problem with shell model calculations,[25–27] which generally predict static quadrupole moments for the ^{22}Ne 2_1^+ state that are considerably smaller than experi-

TABLE II. Optical model deformation parameters for 0^+, 2_1^+, and 4_1^+ coupled-channels fits to ^{20}Ne (131 MeV) and ^{22}Ne (132 MeV) scattering from ^{208}Pb. Real, imaginary, and spin-orbit potentials were taken to have the same deformation parameters.

	β_2^c	β_4^c	β_2^N	β_4^N
^{20}Ne	0.421	0.25	0.139	0.033
^{22}Ne	0.440	−0.05	0.132	−0.028

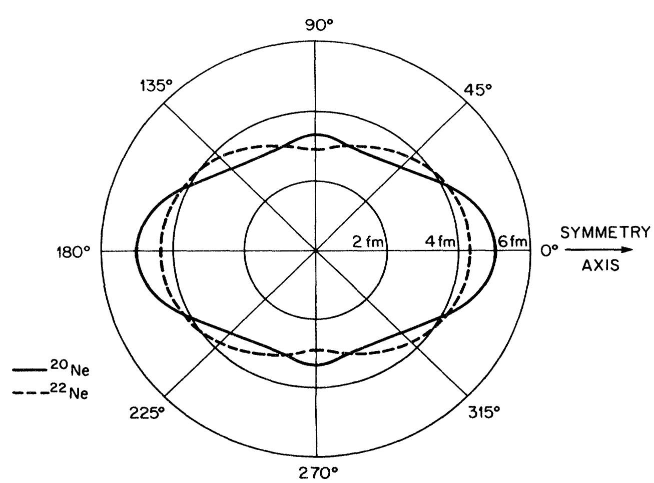

FIG. 4. Nuclear charge shapes for ^{20}Ne and ^{22}Ne implied by the parameters of Table II where the charge surface for mass A is given by

$$R_A^c(\theta) = 1.25A^{1/3}[1 + \beta_2^c Y_{20}(\theta) + \beta_4^c Y_{40}(\theta)] .$$

TABLE III. Transition matrix elements for 0^+, 2_1^+, and 4_1^+ coupled-channels fits to ^{22}Ne (131 MeV) and ^{20}Ne (132 MeV) scattering from ^{208}Pb. $M(E2;4_1^+\text{-}4_1^+)$ was taken to have the rotational model value. Signs correspond to the sign convention employed in the coupled channels program ECIS (Ref. 17).

	$M(E2;0^+\text{-}2_1^+)$ (e b)	$M(E4;0^+\text{-}4_1^+)$ (e b^2)	$M(E2;2_1^+\text{-}2_1^+)$ (e b)	$M(E2;2_1^+\text{-}4_1^+)$ (e b)	Reference
^{20}Ne	−0.180	+0.023	+0.36	−0.22	2, this work
^{22}Ne	−0.144 ±0.005	−0.0033 ±0.003	+0.38 ±0.07	−0.20 ±0.04	this work
	−0.165 ±0.01				19
		+0.01			22
				0.239[a] ±0.005	20
			+0.24 ±0.05		21
			+0.28 ±0.05		24
			+0.19 ±0.01		25–27 shell model

[a]Sign not determined in lifetime measurement (Ref. 20).

ment. A similar problem has been noted previously[2] for ^{20}Ne.

IV. COMPARISON WITH ^{20}Ne

The apparent need for a spin-orbit term to account for ^{22}Ne inelastic data prompted a reexamination of the previous analysis[2] for the system ^{20}Ne(131 MeV) + ^{208}Pb. This reexamination has led to a slightly better fit to the ^{20}Ne data, not by the addition of a spin-orbit potential but by a slightly larger hexadecapole charge deformation ($\beta_4^c=0.25$ instead of the previous[2] $\beta_4^c=0.225$) and by allowing the nuclear quadrupole deformation β_2^N to vary from the rolling-model prescription.[23] The improved fit to the ^{20}Ne data is represented by the dotted curves in Figs. 1 and 2 and the corresponding parameters are presented in Tables I–III. It is worth noting that two extra valence neutrons in ^{22}Ne relative to ^{20}Ne appear to require a spin-orbit potential to account for an inelastic scattering feature. This is reminiscent of ^{18}O(120 MeV) + ^{208}Pb scattering,[14] where a spin-orbit potential ($V_{LS}=-0.15$ MeV) was introduced to account better for the observed m-substate populations for the ^{18}O 2_1^+ state. Similarly, ^{18}O has two valence neutrons outside of a closed ^{16}O core. An explanation of this effect may be contained in the cluster properties[9,28] of the involved wave functions.

Finally, we compare the nuclear charge shapes of ^{20}Ne and ^{22}Ne implied by the symmetric rotational-model parameters of Tables I and II. The comparison is shown in Fig. 4. The addition of two neutrons to ^{20}Ne apparently eliminates the equatorial hexadecapole bulge.

V. CONCLUSIONS

In summary, we have provided new elastic and inelastic scattering data for the system ^{22}Ne + ^{208}Pb at the same c.m. energy (120 MeV) as for a previous study[2] of the system ^{20}Ne + ^{208}Pb. Subjecting the new data to a coupled channels analysis suggests the need for a small negative spin-orbit potential to account for the ^{22}Ne 2_1^+ state cross section near the grazing angle. The extracted matrix elements and deformation parameters for ^{22}Ne are compared to those for ^{20}Ne which were obtained in a completely analogous fashion. Both nuclei appear to have very large static quadrupole moments for their 2_1^+ states, which poses a problem for the shell model.[25–27] Both nuclei have large prolate deformations. In addition, ^{20}Ne has a large positive hexadecapole for its charge distribution, whereas ^{22}Ne, if it has any, has a small negative hexadecapole deformation.

Oak Ridge National Laboratory is operated by Union Carbide Corporation under Contract No. W-7405-eng-26 with the U. S. Department of Energy.

[1]D. L. Hillis, E. E. Gross, D. C. Hensley, C. R. Bingham, F. T. Baker, and A. Scott, Phys. Rev. C 16, 1467 (1977).
[2]E. E. Gross, T. P. Cleary, J. L. C. Ford, D. C. Hensley, and K. S. Toth, Phys. Rev. C 17, 1665 (1978).
[3]J. X. Saladin, I. Y. Lee, R. C. Haight, and D. Vitoux, Phys. Rev. C 14, 992 (1976).
[4]E. E. Gross and M. P. Fewell, Nucl. Phys. A411, 329 (1983).
[5]F. T. Baker, A. Scott, T. P. Cleary, J. L. C. Ford, Jr., E. E.

Gross, and D. C. Hensley, Nucl. Phys. A321, 222 (1979).
[6]J. Nurzynski, C. H. Atwood, T. R. Ophel, D. F. Hebbard, B. A. Robson, and R. Smith, Nucl. Phys. A399, 259 (1983).
[7]F. T. Baker, A. Scott, T. H. Kruse, W. Harting, E. Ventura, and W. Savin, Phys. Rev. Lett. 37, 193 (1976).
[8]S. Landowne and H. H. Wolter, Phys. Rev. Lett. 43, 1233 (1979).
[9]H. Nishioka, R. C. Johnson, J. A. Tostevin, and K.-I. Kubo, Phys. Rev. Lett. 48, 1795 (1982).
[10]G. R. Satchler, in *Proceedings of the International Conference on Reactions between Complex Nuclei,* edited by R. L. Robinson, F. K. McGowan, J. B. Ball, and J. H. Hamilton (North-Holland, Amsterdam, 1974), Vol. 2, p. 171.
[11]W. G. Love, T. Terasawa, and G. R. Satchler, Phys. Rev. Lett. 39, 6 (1977).
[12]A. J. Baltz, P. D. Bond, J. D. Garrett, and S. Kahana, Phys. Rev. C 12, 136 (1975).
[13]W. Weiss, P. Egelhof, K. D. Hildenbrand, D. Krassen, M. Makowska-Rzeszutko, D. Fick, H. Ebinghaus, E. Steffens, A. Amakawa, and K. I. Kubo, Phys. Lett. 61B, 237 (1976).
[14]E. E. Gross, J. R. Beene, K. A. Erb, M. P. Fewell, D. Shapira, M. J. Rhoades-Brown, G. R. Satchler, and C. E. Thorn, Nucl. Phys. A401, 362 (1983).
[15]W. von Oertzen, E. R. Flynn, J. C. Peng, J. W. Sunier, and R. E. Brown, Z. Phys. A 301, 365 (1981).
[16]J. B. Ball, C. B. Fulmer, E. E. Gross, M. L. Halbert, D. C. Hensley, C. A. Ludemann, M. J. Saltmarsh, and G. R. Satchler, Nucl. Phys. A252, 208 (1975).
[17]J. Raynal (private communication).
[18]P. M. Endt and C. Van der Leun, Nucl. Phys. A310, 1 (1978).
[19]X. K. Maruyama, F. J. Kline, J. W. Lightbody, S. Penner, W. J. Briscose, M. Lunnon, and H. Grannel, Phys. Rev. C 19, 1624 (1979).
[20]L. P. Ekström, D. E. C. Scherpenzeel, G. A. P. Engelbertink, H. J. M. Aarts, and H. H. Eggenhuisen, Nucl. Phys. A295, 525 (1978).
[21]D. Schwalm, A. Bamberger, P. G. Bizzeti, B. Povh, G. A. P. Engelbertink, J. W. Olness, and E. K. Warburton, Nucl. Phys. A192, 449 (1972).
[22]R. de Swiniarski, F. G. Resmini, D. L. Hendrie, and A. D. Bacher, Nucl. Phys. A261, 111 (1976).
[23]D. L. Hendrie, Phys. Rev. Lett. 31, 478 (1973).
[24]K. Nakai, F. S. Stephens, and R. M. Diamond, Nucl. Phys. A150, 114 (1970).
[25]M. R. Gunye, Phys. Lett. 37B, 125 (1971).
[26]A. Arima, M. Sakakura, and T. Sebe, Nucl. Phys. A170, 273 (1971).
[27]B. M. Preedom and B. H. Wildenthal, Phys. Rev. C 6, 1633 (1972).
[28]P. J. Moffa, Phys. Rev. C 16, 1431 (1977).